Hypocenter location errors of microseismic events located by using a 3-C VSP downhole geophone array at Violet Grove

Zuolin Chen and Robert R. Stewart

ABSTRACT

Detection of passive microseismic events in oil reservoirs is often accomplished by using an array of subsurface receivers. The location of these events is often determined by a technique which combines arrival times and back-azimuth. However, the accuracy of hypocenter location is difficult to estimate due to the straight line geometry. Also, due to the close distances of events and the effect of nonlinearity on travel times, the error distribution can not be evaluated by the conventional generalized inverse method. Hence, we developed an alternate method to estimate the error distribution, subject to some pre-conditions, by numerical experiments. We estimate that vertical and radial errors are about 10% of the distance of the array from the events. More geophones in the array or wider geophone spacing decreases the location errors. The results may provide some guidelines for the future design of VSP monitoring arrays.

INTRODUCTION

Hypocenter location of a passive microseismic event in oil reservoirs is often accomplished by using a technique which combines the information of back-azimuth and P-wave first arrival times of the event recorded by the 3-C geophones of a VSP array (Oye and Roth, 2003; Phillips et al., 1998). The problem of optimizing a seismic array to obtain information on microseismic events cost-effectively and with high precision is of special importance.

However, the hypocenter location error distribution in this method has rarely been analyzed systematically. In this paper, we try to estimate the error distribution, under some pre-conditions, by numerical experiments; and to provide some guidelines for the future design of VSP downhole geophone arrays.

METHODOLOGY

Hypocenter location

A comparatively detailed description of the previously mentioned hypocenter location algorithm is shown in Figure 1. The back-azimuth of an event defines a vertical plane through the VSP downhole array that contains the source location. The back-azimuth is determined by a best fit solution to the microseismic data using hodogram analysis methods for the P-waves, by using a time window containing the first cycle of the impulsive P-wave first arrival (Flinn, 1965; Vidale, 1986). Hodogram linearity is used as an estimate of the accuracy of the back-azimuth measurement (Vidale, 1986).

After the determination of the back-azimuth of the event, hypocenter location is carried out within the vertical plane. Generally, a layered velocity model is used for hypocenter location. As most VSP downhole geophone arrays are deployed close to the oil reservoir to monitor the passive microseismic activity, the P-wave velocity is often assumed to be constant between the top and bottom geophones. Using a least squares method, the *RMS* of the differences between observed and calculated arrival times is minimized. The picking accuracy of the P-wave first arrival times depends on many factors, such as sampling rate, *S/N* ratio, and slope of an impulsive first arrival.

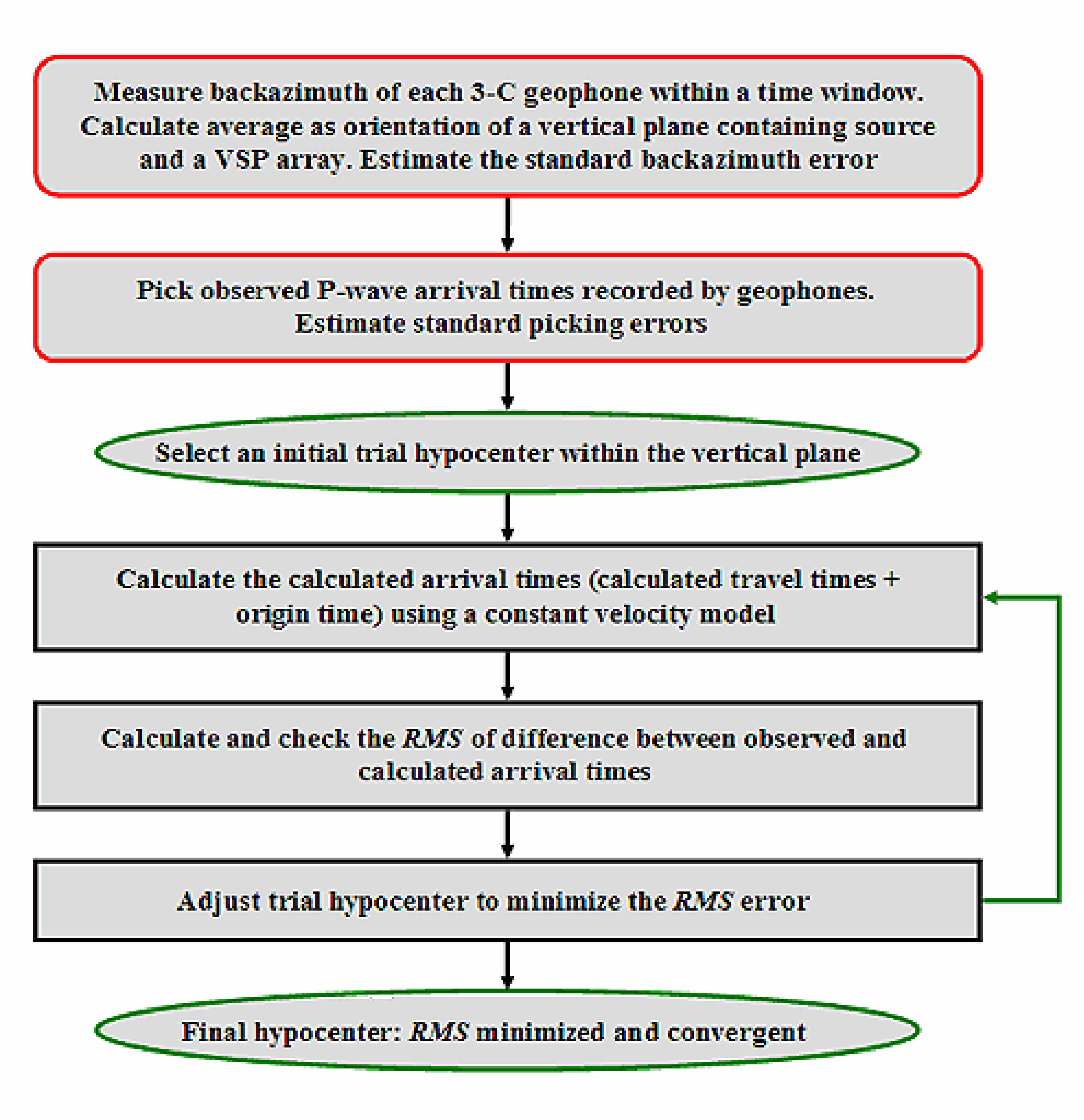

FIG. 1. Flow chart for the hypocenter location algorithm based on back-azimuth and P-wave first arrival time inversion.

For convenience, the hypocenter location error is defined in cylindrical coordinates by the back-azimuth (transverse,T), the depth below the surface of the earth (Z), and the radial distance (R) between the source location and the VSP geophone array. The corresponding hypocenter location of an event *j* (β_j, L_j, and Z_j) is illustrated in Figure 2.

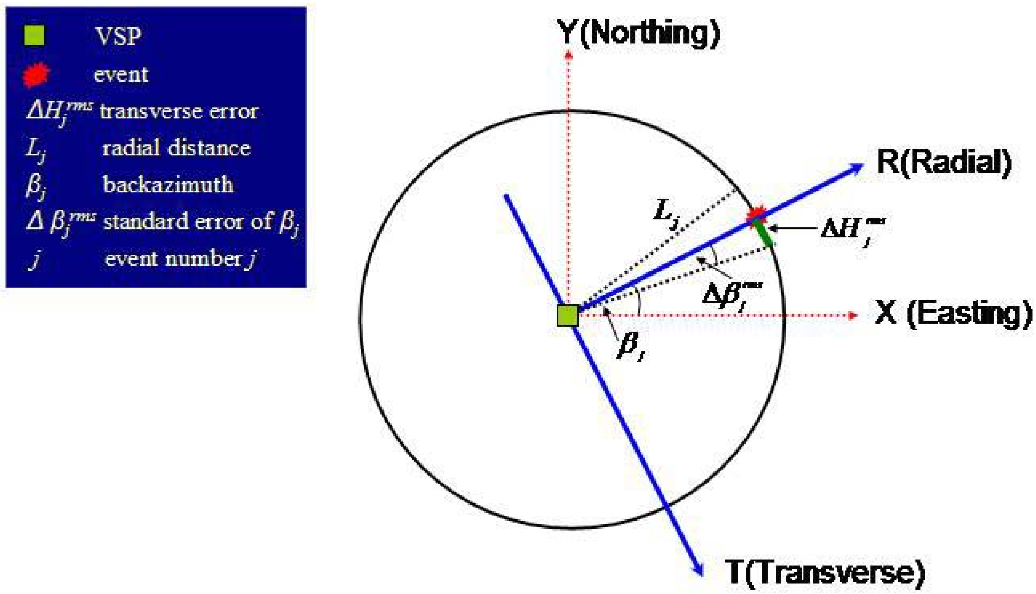
VSP
event
ΔH_j^{rms} transverse error
L_j radial distance
β_j backazimuth
$\Delta\beta_j^{rms}$ standard error of β_j
j event number j
Y(Northing)
R(Radial)
L_j
ΔH_j^{rms}
$\Delta\beta_j^{rms}$
X (Easting)
β_j
T(Transverse)

(a)

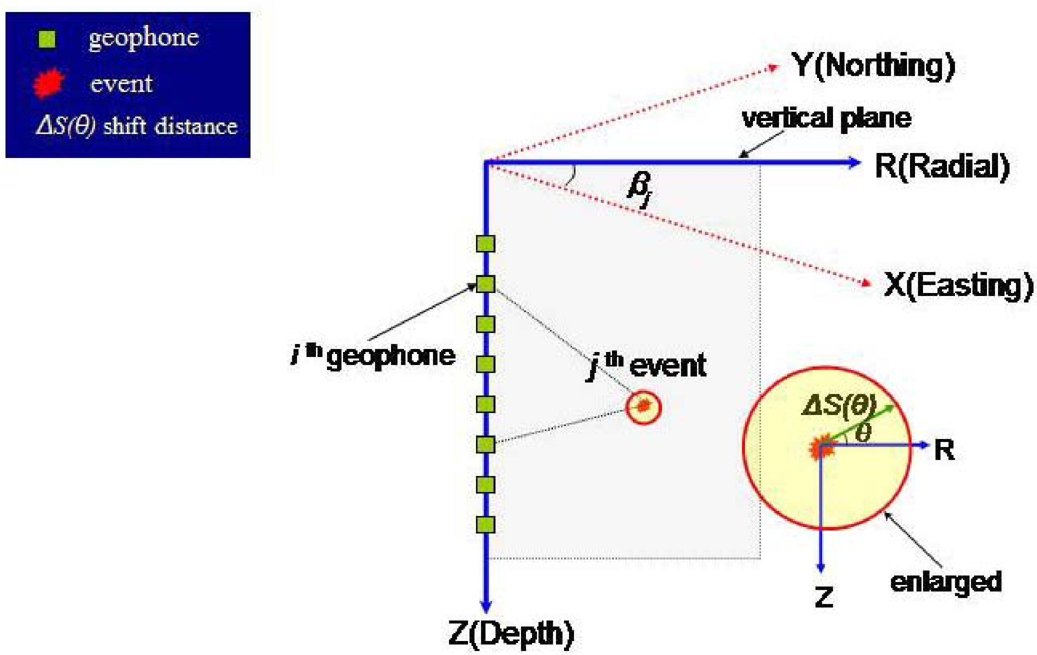
geophone
event
$\Delta S(\theta)$ shift distance
Y(Northing)
vertical plane
R(Radial)
β_j
X(Easting)
i^{th} geophone
j^{th} event
$\Delta S(\theta)$
θ
R
Z
enlarged
Z(Depth)

(b)

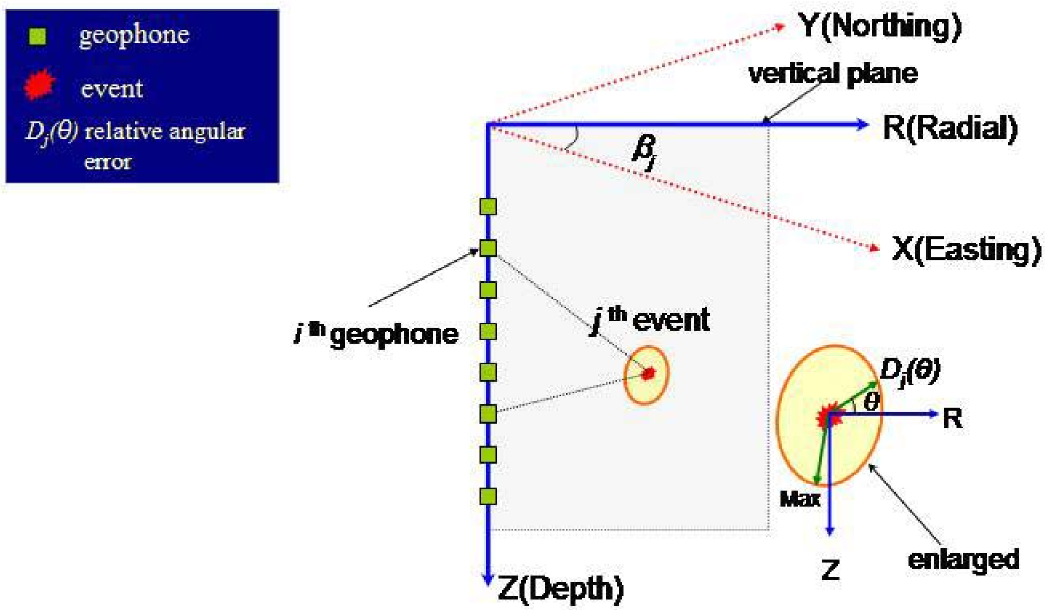

(c)

FIG. 2. (a) Plan view of the cylindrical coordinates used in the calculation of the transverse hypocenter location error ΔH_j. (b) 3-D view of a small shift distance $\Delta S(\theta)$ of assumed hypocenter around real event within the vertical plane. The assumed hypocenters form a circle around the real events. (c) 3-D Illustration of the corresponding relative hypocenter location error $\Delta D(\theta)$ calculated by shifting the assumed hypocenter around real event within the vertical plane. The trace of $\Delta D(\theta)$ is similar to an ellipse with a maximum value.

Error in the transverse direction

From geometry (Figure 2), we see that the hypocenter location error in the transverse direction, ΔH_j is related to the accuracy of back-azimuth and the radial distance of the microseismic event with respect to the VSP array. Suppose the standard back-azimuth error of the event determined by geophone i to be $\Delta\beta_{ij}$. Then the corresponding *RMS* error for the whole geophone array ($\Delta\beta_j^{rms}$) is given by

$$\Delta\beta_j^{rms} = (\sum_{i=1}^{m} \Delta\beta_{ij}^2 / m)^{1/2} , \qquad (1)$$

where m denotes the number of geophones in the VSP array.

Using this value, the standard hypocenter location error in the transverse direction can be simply estimated from the following equation

$$\Delta H_j^{rms} = L_j \sin(\Delta \beta_j^{rms}) \qquad (2)$$

Error within the vertical plane

Hypocenter location errors within the vertical plane are due to the random picking error of the P-wave first arrival times, and systematic arrival time errors due to the difference between real and assumed velocity models. The conventional hypocenter location error estimate is generally performed by using the covariance matrix of an error ellipse after the hypocenter location procedure.

In a typical hypocenter inversion procedure, an optimal hypocenter is determined by minimizing the sum of squared first arrival time residuals (*SSR*) in a least squares method:

$$SSR_j = \sum_{i=1}^{m} (t_{ij}^{obs} - t_{ij}^{cal})^2 \ . \qquad (3)$$

where t_{ij}^{obs}, t_{ij}^{cal} and t_{ij}^{obs}-t_{ij}^{cal} denote the observed first arrival times, the corresponding calculated arrival times, and the time residual at the geophone i^{th} respectively; m is the number of geophones.

In contrast to the previous time residual error estimation method, which assumes a prior picking error to each first arrival time, and then produces error ellipse (Evernden, 1969), this new error estimation algorithm is established in a reversed way. The basic aim is to determine the in-plane angular variation due to the dislocation of the hypocenter, as shown in the following steps:

First, when there is no picking error and the assumed velocity model matches the real one, a hypocenter will be located at its real location, and the time residual will be zero. Suppose due to the picking errors of first arrival times, a hypocenter is located a small fixed distance (ΔS) away from its real location, and hence the possible calculated hypocenters form a circle of radius ΔS around the real one (Figure 2). The $SSR_j(\theta)$ of any point on the circle is calculated based on its location, the geometry of the VSP array, and the local velocity, where θ is the angle from the center to the point.

By taking the square root of the average of $SSR_j(\theta)$, a normalized $SSR_j^{norm}(\theta)$ is obtained by

$$SSR_j^{norm}(\theta) = (\sum_{i=1}^{m} SSR_{ji}(\theta)/m)^{1/2} \ . \qquad (4)$$

Clearly, $SSR_j^{norm}(\theta)$ represents the normalized *RMS* of the whole time residuals, and inherits the same physical meaning. Conversely, we defined another index, $\Delta D_j(\theta)$, by using the ratio between ΔS and $SSR_j^{norm}(\theta)$ as follows:

$$\Delta D_j(\theta) = \Delta S / SSR_j^{norm}(\theta)\ . \tag{5}$$

Here $\Delta D_j(\theta)$ indicates the distance shift with the change of a unit of $SSR_j^{norm}(\theta)$ residuals (1ms) due to the picking errors. It reflects the shape of the error distribution around the real hypocenter.

NUMERICAL EXPERIMENTS AND RESULTS

Data and pre-conditions

The model of the downhole VSP array used for estimating hypocenter location errors in this study is based on a VSP monitoring survey carried out in Violet Grove near Drayton Valley, Alberta, for a CO_2 EOR and storage study (Lawton et al., 2005).

The VSP geophone array consists of eight 3-C geophones deployed from approximately 1500m to 1640m in depth. The P-wave velocity close to the oil reservoir is approximately 4000 m/s based on surface reflection data.

Numerical experiments are accomplished based on the following pre-conditions:

1. The standard back-azimuth error of each of the eight geophones is assumed to vary randomly from 0° to 5°.

2. The standard picking error of P-wave first arrival time, Δt_{ij}^{pick}, is estimated to be less than 2ms.

3. There is no difference between the assumed and real velocity models. Thus, P-wave arrival times are only affected by the random picking error.

Error distribution in the transverse direction

The general distribution of hypocenter location errors in the transverse direction is calculated and depicted by assigning the locations of events distributed at intervals of 5m (Figure 3). Note that due to the random variation of the standard backa-zimuth of geophone, errors fluctuate even though the radial distances are the same. The fluctuations become more severe as the radial distance increases. In general, the hypocenter location error in the transverse direction shows a trend of a series of concentric circles around the VSP array.

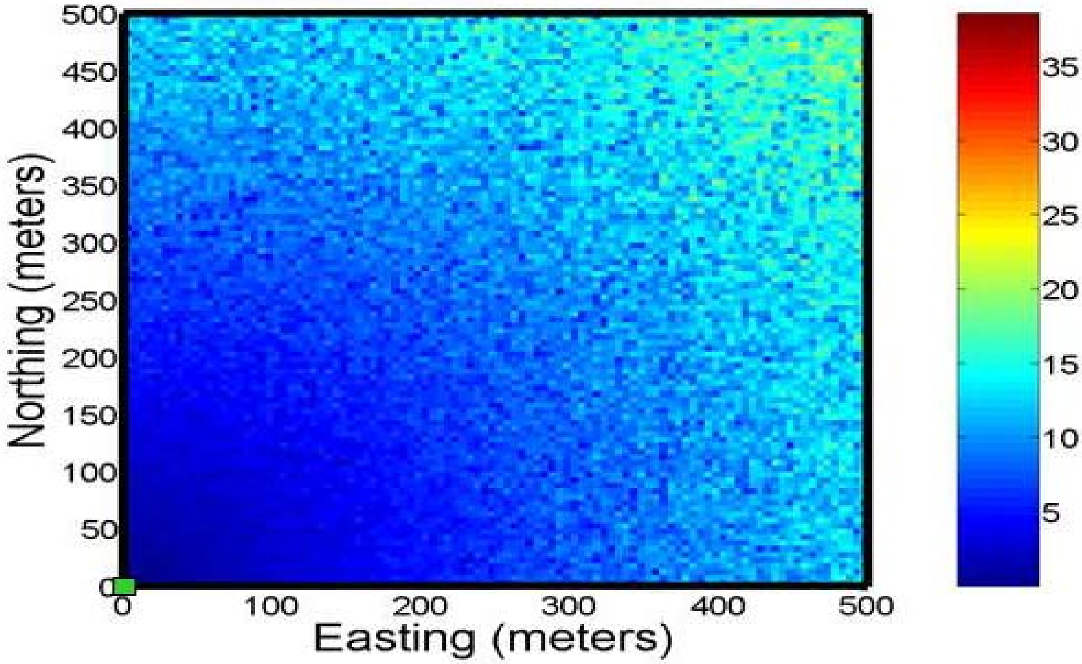

(a)

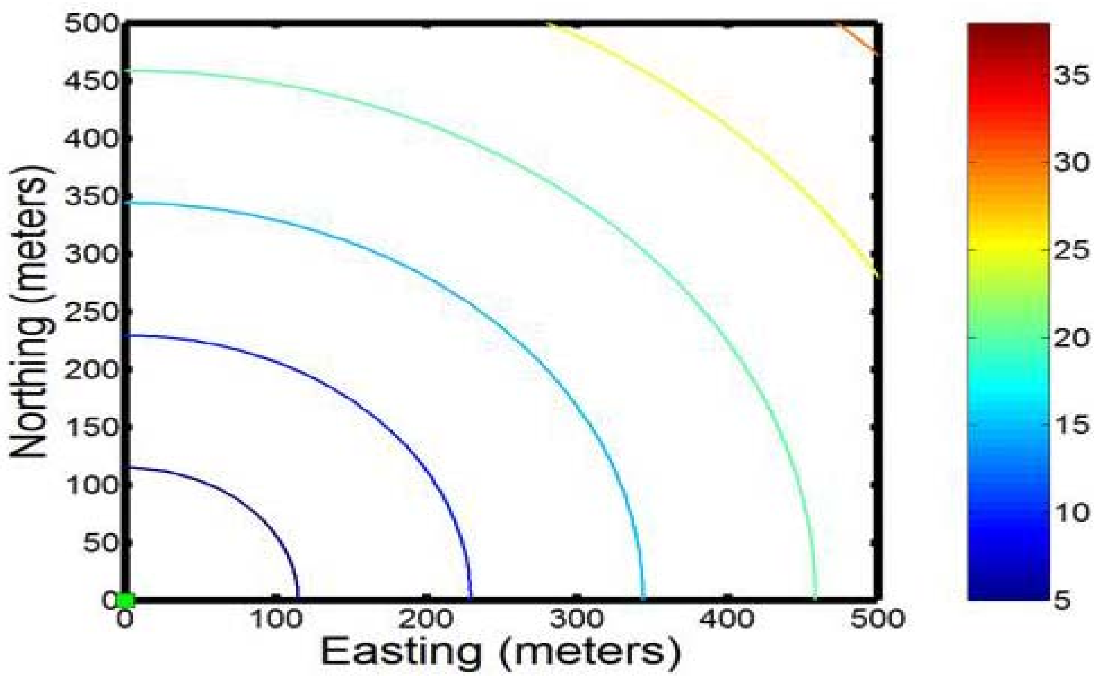

(b)

FIG. 3. (a) Distribution of hypocenter location errors in the transverse direction with random backazimuth errors ranging from 0° to 5°. (b) Contour map of the hypocenter location errors with backazimuth errors fixed at 2.5°.

Microearthquakes are distributed at 5m intervals; the projection of the VSP array to the surface is marked by a green square. Errors are shown in metres.

Error distribution within the vertical plane

Statistical distributions of hypocenter location errors within the vertical plane are carried out by assigning the locations of events distributed at 20m intervals. Figure 4 shows the orientations and the configuration of hypocenter location errors around the assumed events, where ΔS is calculated to be 8m based on the assumed picking error (less than 2ms) and a P-velocity of 4000 m/s. The orientations and the corresponding values of the hypocenter location errors vary with both the radial and depth directions. The most obvious features of the error distribution are summarized as: both the radial and depth errors of the events are smallest close to the lateral side of the VSP array; with increasing radial distance, depth errors become dominant while the radial errors change little in value. When events occur straight above or below the VSP array, the radial errors are large and increases rapidly with the distance from the nearest geophone. The contour map also shows the maximum error distributions located by the VSP array. In this case, the extent of the reference contour approximately coincides with the depth range of the VSP array.

DISCUSSION

Effect of the number of geophones in a VSP array on hypocenter location errors

Although a VSP array with a large number of geophones is likely to enhance the accuracy of hypocenter location, costs will increase correspondingly. Suppose the picking errors of the P-wave first arrival times and back-azimuths follow a Gaussian normal distribution. According to the central limit theorem of statistics, the relationship between the number of geophones deployed and the confidence interval of the back-azimuth β (that is the orientation of the vertical plane) is $\pm\beta/m^{1/2}$. This relationship states that when the number of geophones in a VSP array surpasses eight, the confidence interval will be reduced by more than half. Another merit of using numerous geophones is that they provide more options for selecting better back-azimuth and first arrival time data, and for excluding those with larger deviations. No doubt, this will increase the accuracy of hypocenter locations and lower the error estimates.

VSP geophone arrays and hypocenter location errors

The depth range of the VSP array, or the distance between the top and bottom geophones, affects the hypocenter location errors within the vertical plane.

To examine the effect of the depth range, we increase the interval between the eight geophones in the VSP array from 20m to 30m, and calculate the error distributions (Figure 5). Although the pattern of orientations of errors remains similar to the previous one, the errors are reduced both laterally and vertically. The depth range of the selected reference contour coincides with the depth range of the larger VSP array. Thus, a VSP array with a larger depth range can lower the hypocenter errors within the vertical plane.

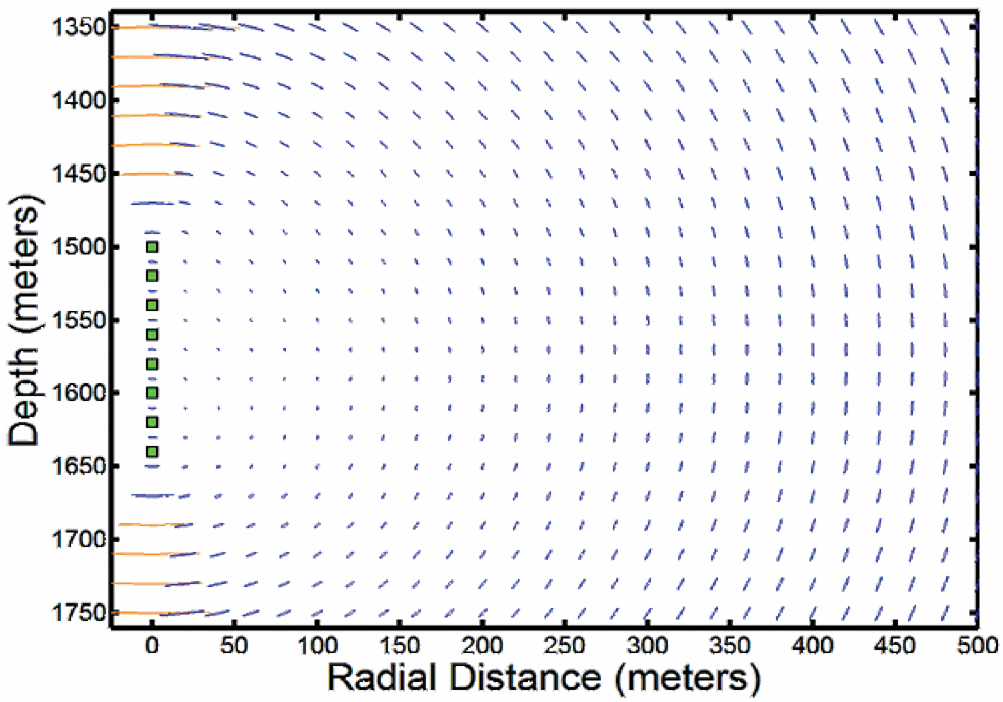

(a)

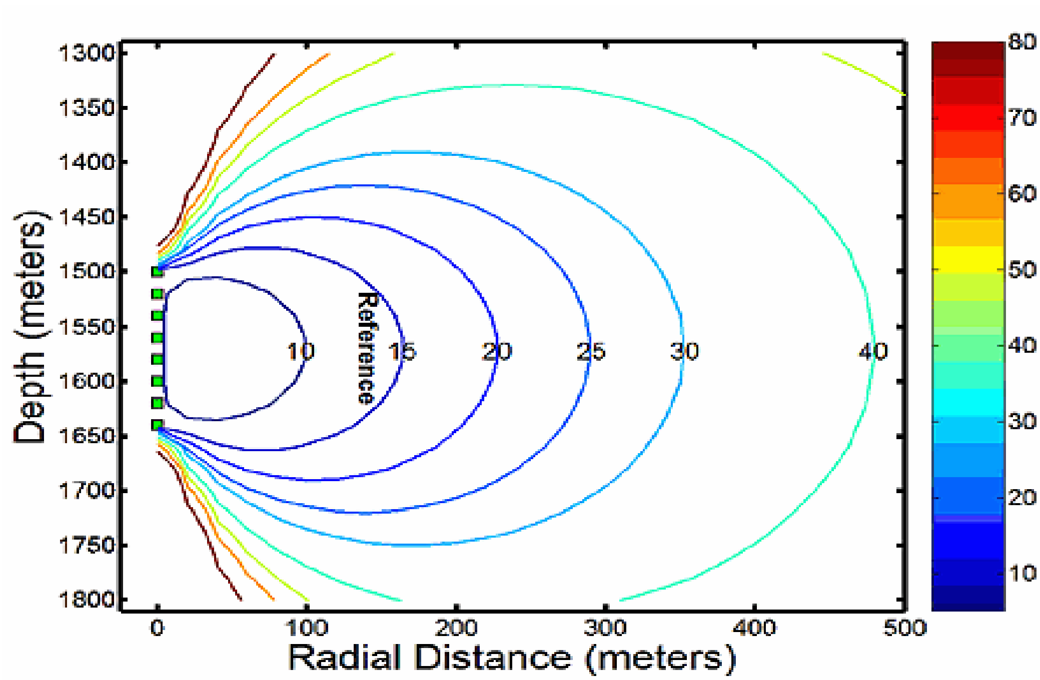

(b)

FIG. 4. (a) the orientations and hypocenter location errors within the vertical plane. For clarity, error values are reduced 8 times, and some very large errors are marked in orange. (b) Contour map of the maximum hypocenter location errors at aligned points. The depths of the geophones of the VSP array are shown on the left side by green squares. Errors are shown in metres.

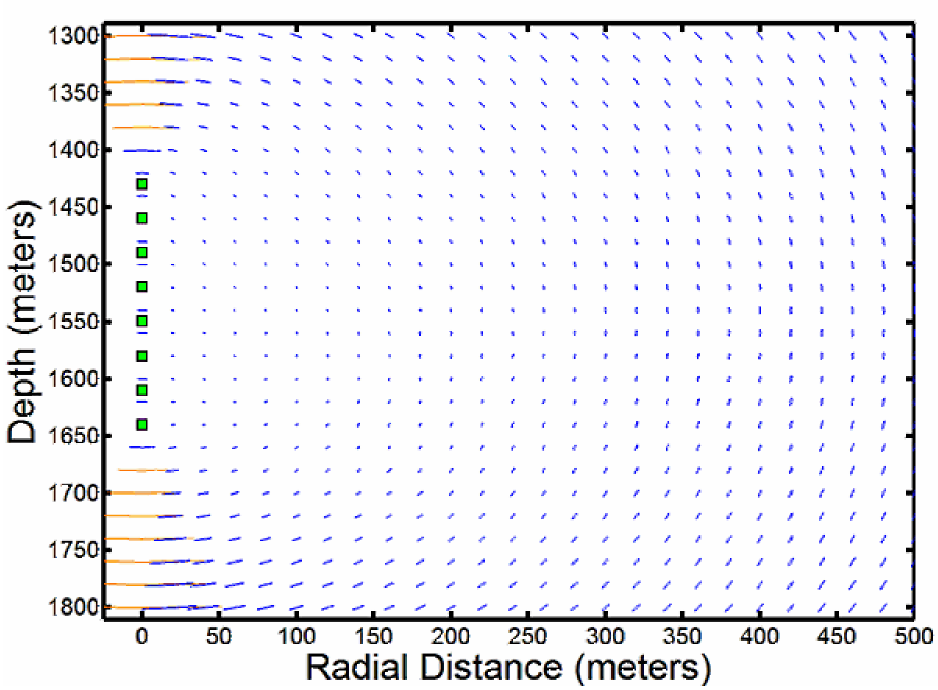

(a)

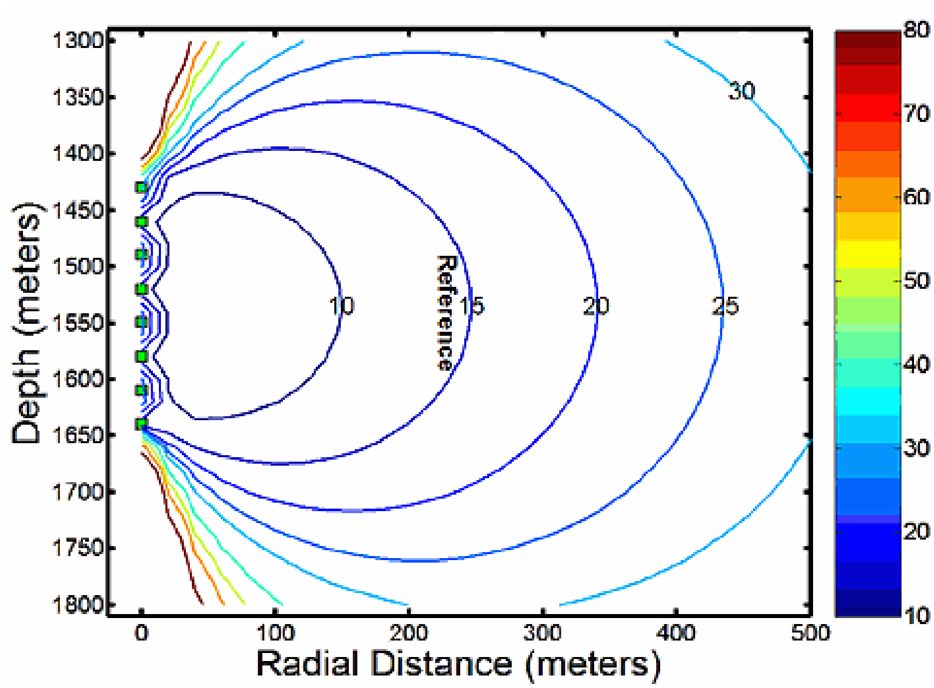

(b)

FIG. 5. (a) the orientations and hypocenter location errors within the vertical plane calculated by the larger depth range VSP array. For clarity, error values are reduced 8 times, and some very large errors are marked in orange. (b) Contour map of the maximum hypocenter location errors at aligned points. The depths of the geophones of the VSP array are shown on the left side by green squares. Error is shown in metres.

CONCLUSIONS

There are many factors which affect the distribution of hypocenter location errors located by using a VSP geophone array. In these numerical experiments, hypocenter location errors expressed in local cylindrical coordinates are estimated and summarized as follows:

1. The hypocenter location error in the transverse direction is proportional to the standard back-azimuth error and the radial distance of an event with respect to the VSP array.

2. Within the vertical plane, the orientations and the corresponding values of the hypocenter location errors vary with both the radial and depth directions. Both the radial and depth errors of the events are smallest near the lateral side of the VSP array. The depth errors increase with radial distance, while radial errors become worst when events occur straight above or below the VSP array.

3. The depth range of reference contour approximately coincides with the depth range of the VSP array. Presumably, a VSP array with a large depth range of geophones can extend the small-error area.

4. The number of geophones deployed in a VSP array can reduce the confidence interval of the orientation of the vertical plane. In addition, numerous geophones can provide more options for selecting better back-azimuth and first arrival time data and excluding larger deviation ones, and hence reduce the errors of hypocenter locations.

ACKNOWLEDGEMENTS

The authors thank Kevin Hall and Rolf Maier of the CREWES project.

REFERENCES

Bondár, I., S. C. et al., 2004, Epicentre accuracy based on seismic network criteria: Geophys. J. Int., **156**, 483–496.

Evernden, J., 1969, Precision of epicenters obtained by small numbers of world-wide stations: Bull. Seismol. Soc. Am. **59**, 1365–1398.

Flinn, E.A., 1965, Signal analysis using rectilinearity and direction of particle motion: Proc.IEEE, **53**, 1874-1876.

Lawton et al., 2005, Overview of the Violet Grove CO2 seismic monitoring project. CREWES Report, Univ. of Calgary, **58**, 1-24

Oye, V. and Roth, M., 2003, Automated seismic event location for hydrocarbon reservoirs: Computers & Geosciences, **29**, 851-863.

Philips, W.S. et al., 1998, Induced microearthquake patterns in oil-production fracture systems in the Austin chalk: Tectonophysics, **289**, 153–169.

Vidale, J.E.,1986, Complex polarization analysis of particle motion: Bull. Seismol. Soc. Am. **76**, 1393–1405.